Transactions on Modelling and Simulation vol 16, © 1997 WIT Press, www.witpress.com, ISSN 1743-355X

Numerical Simulation of Vortex Shedding from an Oscillating Circular Cylinder

J. R. Meneghini*, F. Saltara* & P. W. Bearman**
**University of São Paulo, EPUSP, Department of Mechanical Engineering, CEP 05508-900, São Paulo, SP Brazil*
EMail: jmeneg@ usp. br
***Imperial College of Science, Technology & Medicine, Department of Aeronautics, London, SW7 2BY, UK*
EMail: p.bearman@ic.ac.uk

Abstract

The interaction between cylinder oscillation and the shedding of vortices is investigated numerically in this paper. The near wake structure is presented for different values of reduced velocity of a cylinder free to oscillate transversely. One of the objectives of this paper is to compare the numerical results with experimental data obtained by Parra [11] in the water tank facility of IPT/University of São Paulo. The attraction of applying numerical methods to this problem is that the way the flow is modified can be studied in closer detail. In the computer it is possible to investigate many different flow conditions more easily.
The method used for the simulation is based on the Vortex-in-Cell formulation incorporating viscous diffusion. The Navier-Stokes equations are solved using the operator-splitting technique, where convection and diffusion of vorticity are treated separately. The convection part is modelled assuming that the vorticity field is carried on a large number of discrete vortices. Force coefficients are calculated by considering the normal gradient of vorticity at the wall to evaluate the pressure contribution and the vorticity at the wall to obtain the skin friction.

1 Introduction

Many investigations of the effect of transverse oscillations on vortex shedding can be found in the literature. It is observed that sinusoidal transverse oscillations are characterised by the capture of the vortex shedding frequency by the oscillation frequency over a range of cylinder oscillation amplitudes.

Transactions on Modelling and Simulation vol 16, © 1997 WIT Press, www.witpress.com, ISSN 1743-355X

This phenomenon is called *lock-in*. Meneghini and Bearman [8] investigated square, saw-tooth and parabolic wave forms of cylinder transverse oscillations, and found that only for a parabolic wave did *lock-in* occur in a similar way to that observed with sinusoidal oscillation.

With a cylinder free to oscillate, the *lock-in* phenomenon is characterised by the capture of the vortex shedding frequency by the natural frequency of the cylinder, over a range of reduced velocities. Results by Brika and Laneville [3] and Parra [11] show that in the region of *lock-in* large amplitudes of oscillation are observed for high mass parameter values, with the mass parameter defined by equation (11). According to Blevins [2] and others, large amplitude vibration increases the correlation of vortex shedding along the cylinder axis. With this consideration, two-dimensional numerical simulations should be reliable in terms of analysing flow details and wake structures in the *lock-in* regime.

In this work the vortex shedding from a cylinder free to oscillate transversely is investigated numerically. The results are compared with the experimental data obtained by Parra [11] and Khalak and Williamson [5]. The method used for the simulations is based on the Vortex-in-Cell formulation incorporating viscous diffusion. The Navier-Stokes equations are solved using the operator-splitting technique, where convection and diffusion of vorticity are treated separately. The convection part is modelled assuming that the vorticity is carried on a large number of discrete vortices. Force coefficients are calculated by considering the normal gradient of vorticity at the wall to evaluate the pressure contribution and the value of the vorticity at the wall to evaluate the skin friction. For each time step, once the force coefficients were calculated, the second order ordinary differential equation for the transverse motion of the cylinder is solved through a Runge-Kutta method. The resulting cylinder velocity is used to obtain the relative free-stream velocity for the next time step.

2 Numerical Method

The Vortex-in-Cell formulation incorporating viscous diffusion has been applied by Meneghini and Bearman to investigate the effect of large amplitude of oscillation on vortex shedding from an oscillating circular cylinder [7] and to investigate the effect of displacement wave form on vortex shedding from a circular cylinder [8]. Arkell et al. [1] used the method to study the effects of waves on the far wake behind a circular cylinder. This approach has been developed by Graham [4] and details about the method can be found in Meneghini and Bearman [6]. A thorough review of vortex methods has been published by Sarpkaya [12].

In order to study the flow about a circular cylinder a conformal transformation $(x,y) \rightarrow (\xi, \eta)$ is used. The cylinder wall is specified by a line $\eta = 0$ in the transformed plane. The two-dimensional Navier-Stokes equations in vorticity (ω) stream function (ψ) formulation in the transformed plane can be written as:

$$J\frac{\partial \omega}{\partial t} - \frac{\partial \psi}{\partial \eta}\frac{\partial \omega}{\partial \xi} + \frac{\partial \psi}{\partial \xi}\frac{\partial \omega}{\partial \eta} = \nu\left(\frac{\partial^2 \omega}{\partial \xi^2} + \frac{\partial^2 \omega}{\partial \eta^2}\right) \tag{1}$$

$$\frac{\partial^2 \psi}{\partial \xi^2} + \frac{\partial^2 \psi}{\partial \eta^2} = -J\omega \tag{2}$$

where ν is the kinematic viscosity and J is the Jacobian of the transformation. Equation (2) represents Poisson's equation for the stream function in the transform plane. Equation (1) is solved using the operator-splitting technique, where convection and diffusion of vorticity are treated separately:

$$\left[J\frac{\partial \omega}{\partial t}\right]_{convection} = -\frac{\partial \psi}{\partial \eta}\frac{\partial \omega}{\partial \xi} + \frac{\partial \psi}{\partial \xi}\frac{\partial \omega}{\partial \eta} \tag{3}$$

$$\left[J\frac{\partial \omega}{\partial t}\right]_{diffusion} = \nu\left(\frac{\partial^2 \omega}{\partial \xi^2} + \frac{\partial^2 \omega}{\partial \eta^2}\right) \tag{4}$$

The convection part is modelled assuming that the vorticity field ω is carried on a large number of discrete vortices. The vorticity is represented by a distribution of discrete vortices in the form:

$$\omega(\xi,\eta,t) = \sum_{k=1}^{Nv} \Gamma_k \delta(\xi - \xi_k(t))\delta(\eta - \eta_k(t)) \tag{5}$$

where Γ_k is the circulation of the kth point vortex, and δ is the Dirac function. Poisson's equation (2) is solved at each time step on a grid which is uniform in the ξ direction so that a Fast Fourier Transform algorithm may be used. A stretched mesh is employed in the η direction in order to resolve accurately the cylinder boundary layer. For the purpose of solving Poisson's equation, circulation of the kth discrete vortex in a mesh cell is projected to the four surrounding mesh points according to a bilinear area weighting scheme. Equation (2) results in a tridiagonal set of equations for the transform of ψ on the η = constant grid lines, after taking a fast discrete Fourier Transform in the ξ direction and using a central difference scheme. The solution of this tridiagonal set of equations gives ψ at every mesh point (i,j) . The velocity components at these points are then calculated by a finite difference scheme applied to the relation between velocity and stream function.

Transactions on Modelling and Simulation vol 16, © 1997 WIT Press, www.witpress.com, ISSN 1743-355X

Boundary conditions on ψ are $\psi = 0$ at the body surface and the value of ψ is evaluated by Biot-Savart integration at the outer boundary of the computational domain. The contribution of the free stream is considered separately. The values of vorticity at the mesh points are considered for the Biot-Savart integration rather than the circulation of each discrete vortex. This is done in order to have a more efficient procedure in terms of computational time.

The diffusion part of equation (1), which is given in (4), is solved by a finite difference scheme in a semi-implicit form carried out on the same fixed expanding mesh as used for convection. The wall vorticity is calculated in order to satisfy the no-slip boundary condition. The solution of (4) gives the change in vorticity due to diffusion at every mesh point. The change in vorticity is projected back on to a point vortex in a similar manner as used by the area weighting scheme. The convection part of the Navier-Stokes equations is satisfied by convecting the point vortices in a Lagrangian way. The velocity components of the *k*th discrete vortex are found by interpolation of the velocities in the four mesh points surrounding this vortex.

3 Force Evaluation

Force coefficients are calculated by suitably integrating the pressure and skin friction contributions. After considering the contributions from skin friction and pressure, the force components are resolved in the two directions *(x,y)* in the physical plane , yielding F_x and F_y. These forces are then non-dimensionalised as follows:

$$Cl = \frac{2F_y}{\rho U^2 D} + \frac{\pi D}{2U^2}\frac{d^2 y}{dt^2} \tag{6}$$

$$Cd = \frac{2F_x}{\rho U^2 D} \tag{7}$$

where ρ is the fluid density, U is the free stream velocity D is the circular cylinder diameter, and y is the position of the cylinder in the transverse direction . The second term on the right side of equation (6) is the correction due to the acceleration of the cylinder in the transverse direction. As our mesh is fixed to the body, this correction must be done to take into account the inertia effect.

4 Equations for Vortex-induced Vibration

The equation of motion for a cylinder free to oscillate in the transverse direction is:

Transactions on Modelling and Simulation vol 16, © 1997 WIT Press, www.witpress.com, ISSN 1743-355X

$$m\ddot{y}+2\beta m\omega_n\dot{y}+m\omega_n^2 y=Cl(t)\rho\frac{U^2}{2}D \qquad (8)$$

where m is the mass of the cylinder per unit length, ω_n is the natural frequency of the cylinder, and β is the fraction of critical viscous damping. According to Parkinson [10], if the non-dimensional transverse displacement of the cylinder given is by $Y=y/D$ and the non-dimensional time is given by $\tau=Ut/D$, then equation (8) can be rewritten as:

$$\ddot{Y}+2\beta\dot{Y}+Y=C_l n\frac{1}{4\pi^2}V_r^2 \qquad (9)$$

where:

$$\ddot{Y}=\frac{d^2Y}{d\tau^2} \quad \text{and} \quad \dot{Y}=\frac{dY}{d\tau}\ , \qquad (10)$$

n, the mass parameter, is given by:

$$n=\frac{\rho D^2}{2m} \qquad (11)$$

and V_r, the reduced velocity, is given by:

$$V_r=\frac{UT_n}{D} \qquad (12)$$

where T_n is the natural period of the cylinder, $T_n=2\pi/\omega_n$.

Once a lift coefficient for a time step is calculated using (6), equation (9) can be solved through a fourth order Runge-Kutta method to give the velocity of the cylinder in the transverse direction. With the cylinder considered fixed on the grid, this velocity is applied to the free stream for the next time step.

5 Discussion of Results and Conclusions

In all numerical results shown in this paper, Re = 200, with the Reynolds number defined in terms of cylinder diameter (D) and free stream velocity (U), $Re=UD/\nu$. A mesh with 170 points in the radial direction and 128 points in the angular direction has been used in all simulations. There are about 30 points in the boundary layer with this mesh. A non-dimensional time step, Ut/D, equal to

0·005 has been used. Lift and drag coefficients, for the case of a fixed circular cylinder at a Reynolds number equal to 200, are shown in figure 1. The wake structure, represented by the point vortices, is shown in figure 2.

In the simulations for Re = 200 vortex shedding occurs with a Strouhal number of about 0·2. This value is very close to those observed in experiments for Re between 200 and about 2 x 10^5. For Re = 200, the wake is still laminar and hence no turbulence model is needed. The non-dimensional parameters n, β and V_r in the simulations have been kept equal to those measured in the experiments of Parra [11].

The experimental results of Parra [11] were obtained in a water tank facility, with a circular cylinder free to oscillate transversely with $\beta = 0{\cdot}01710$ and $n = 0{\cdot}34681$. The experiments were conducted with a circular cylinder of $D = 0{\cdot}11$m and $\omega_n = 2{\cdot}238$ rad/s. The flow velocity U was varied in order to change the reduced velocity. The Reynolds Number Re of the experiments varied in the range 14410 to 50380. In the numerical simulations, the velocity U and diameter D of the cylinder have been fixed for all calculations, and the natural period T_n has been varied to change the reduced velocity. The non-dimensional amplitude of the cylinder transverse oscillation A/D has been plotted as a function of the reduced velocity UT_n/D. The experimental and numerical results can be seen in Figure 9.

Simulations have been carried out for values of reduced velocity, V_r, from 2·0 to 14·0. In figures 3, 4, and 5 force time histories and cylinder displacements are show for V_r equal to 5·0, 7·5 and 12·5, respectively. The highest amplitude of oscillation occurred for a reduced velocity equal to 5·0, and this is also the reduced velocity for the highest value of the mean drag coefficient. As the reduced velocity is increased above 5, the amplitude and mean drag coefficient decrease. The phase angle by which the lift coefficient leads the cylinder displacement changes dramatically as the reduced velocity varies from 5·0 to13·0. This result has been observed in experiments (as can be seen in the review by Parkinson [11]), and also in simulations where the cylinder is forced to oscillate (Meneghini and Bearman [7]). Plots of the wake structure for these cases are shown in figures 6, 7, and 8. The plots are for the moment when the cylinder is in its upper most position. The wake structure for V_r equal to 5·0 has a distinctive pattern with the vortices in the wake exhibiting a large lateral spacing.

The maximum amplitude, non-dimensionalised with the cylinder diameter ($D = 2{\cdot}0$ in our simulations), versus the reduced velocity is plotted in the graph shown in figure 9. The experimental results by Parra [11] and Khalak and Williamson [5] are also shown and compared with the present simulations. As can be noticed, the maximum amplitude from the simulations is considerably lower than those found in the experiments. The reason for this disagreement is not yet known. The explanation could be related to the difference in Reynolds number in the experiments and in our simulations. However, Brika and Laneville [3] and Khalak and Williamson [5] have shown

Transactions on Modelling and Simulation vol 16, © 1997 WIT Press, www.witpress.com, ISSN 1743-355X

from experiments that there may be two possible values for the maximum amplitude associated with either an upper or a lower branch to the amplitude versus reduced velocity curve. Also there is known to be a hystersis associated with moving between the two branches. The values of mass and damping in Khalak and Williamson's experiments are reasonably close to the ones used in the simulations and it is interesting to note that the maximum amplitude for their lower branch is about 0·6, which is similar to the maximum value computed here. Brika and Laneville [3] contend that the mode of shedding is different in the two branches and, following the nomenclature of Williamson and Roshko [13], find the 2S mode in the lower branch and the 2P mode in the upper branch. In the 2S mode two vortices are generated per oscillation cycle and in the 2P mode two vortex pairs are formed per cycle. It is clear from figures 6, 7 and 8 that the computed flow is in the 2S mode, which is compatible with the levels of amplitude predicted. More work is required to determine if the vortex shedding can be encouraged to change into the 2P mode and whether this results in larger amplitudes.

The results shown in this paper are part of a research project that is still been carried out. The next steps will to be investigate whether it is possible to cause the vortex shedding mode to change and to implement the Vortex Method with a turbulence model, hence increasing the maximum Re that would be possible to simulate in the computer.

6 Figures

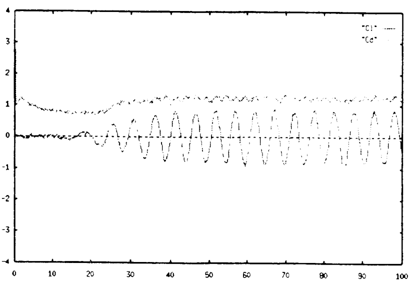

Figure 1 - Force coefficients for *Re*=200

Figure 2- Wake structure for *Re*=200

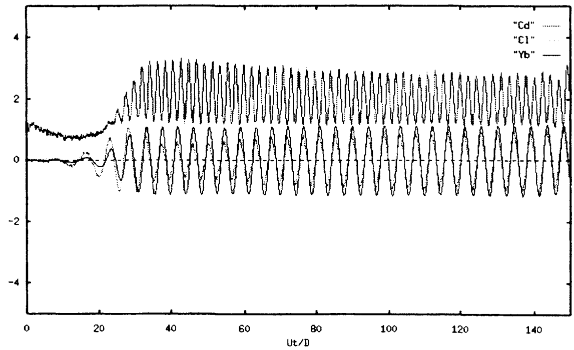

Figure 3 - Results of *Cl, Cd* and *Yb* for UT_n/D =5·0

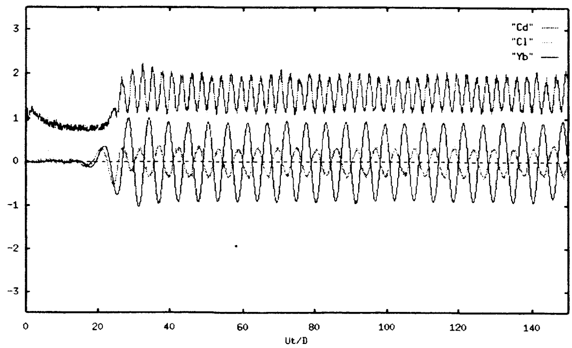

Figure 4 - Results of *Cl, Cd* and *Yb* for UT_n/D =7·5

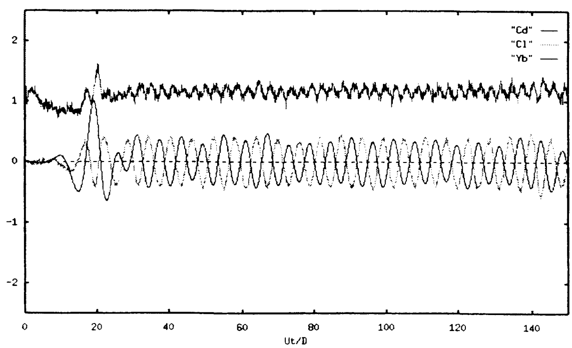

Figure 5 - Results of *Cl, Cd* and *Yb* for UT_n/D =12·5

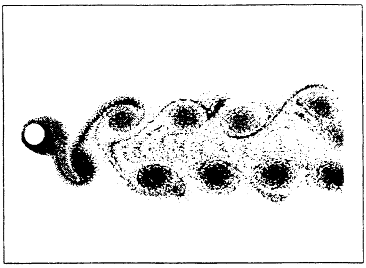

Figure 6 - Wake structure for $UT_n/D=5{\cdot}0$

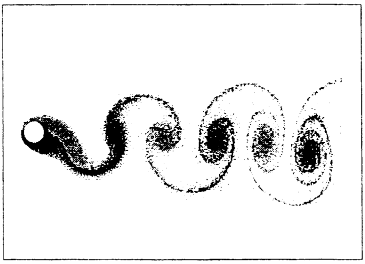

Figure 7 - Wake structure for $UT_n/D=7{\cdot}5$

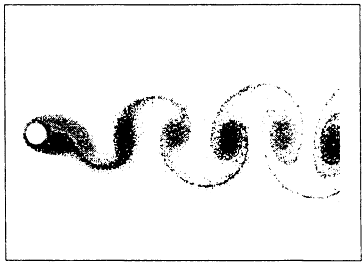

Figure 8 - Wake structure for $UT_n/D=12{\cdot}5$

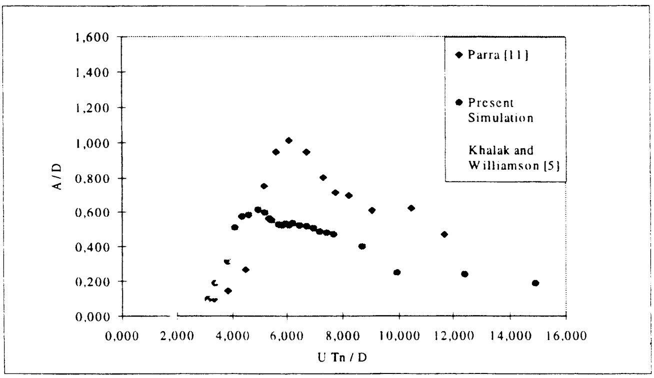

Figure 9 - Non-dimensional amplitude of the circular cylinder transverse oscillation as a function of the reduced velocity

Acknowledgements

The first and second authors (JRM and FS) are grateful to FAPESP (grant 94/3057-0 and 94/3528-3) and CNPq for providing them a Research Grant for this project.

References

1. Arkell, R. H., Graham, J. M. R., and Zhou, C. Y. The effects of waves and mean flow on the hydrodynamic forces on circular cylinders, *Proc. 6th BOSS Conference,* London, 1992.

2. Blevins R. D., *Flow Induced Vibration,* Second edition, Van Nostrand Reinhold, New York, 1990.

3. Brika, D., Laneville, A., Vortex-induced vibration of a long flexible circular cylinder, *Journal of Fluid Mechanics,* Vol. 259, pp. 481-508, 1993.

4. Graham, J. M. R., Computation of viscous separated flow using a particle method, *Numerical Methods in Fluid Mechanics,* Vol.3, pp. 310-317,Ed. K.W. Morton, Oxford University Press, 1988.

5. Khalak, A., and Williamson, C. H. K., Dynamics of a hydroelastic cylinder with very low mass and damping, accepted for publication in the *Journal of Fluids and Structures.*

6. Meneghini, J. R., and Bearman, P. W., Numerical simulation of control of bluff body flow using a discrete vortex method incorporating viscous diffusion, *Proc. IUTAM Symposium on Bluff-Body Wakes, Dynamics and Instabilities,* pp. 257-262, Ed. H. Eckelmann, Springer-Verlag, 1992.

7. Meneghini, J. R., and Bearman, P. W., Numerical simulation of high amplitude oscillatory flow about a circular cylinder, *Journal Fluids and Structures,* Vol. 9, pp. 435-455, 1995.

8. Meneghini, J. R., and Bearman, P. W., Numerical simulation of the interaction between the shedding of vortices and square-wave oscillations applied to a circular cylinder, *Proc. Second International Conference on Hydrodynamics,* Vol. 2, pp.785-790, Ed. Chwang, Lee & Leung, Balkema, Hong Kong, 1996.

9. Meneghini, J. R., Numerical Simulation of Bluff Body Flow Control Using a Discrete Vortex Method, *PhD thesis*, University of London, UK, 1993.

10. Parkinson, G., Phenomena and modelling of flow-induced vibrations of bluff bodies, *Prog. Aerospace Sci.*, Vol. 26, pp. 169-224, 1989.

11. Parra, P. H. C. C., Mod. Semi-empírico de Vib. Ind. por Vortex Shedding - Análise Teórica e Experimental, *MSc Thesis,* University of São Paulo, Brazil, 1996.

12. Sarpkaya, T., Computational methods with vortices - The 1988 Freeman Scholar Lecture, *J. Fluids Engineering,* Vol. 111, pp. 5-52, 1989.

13. Williamson, C.H.K. and Roshko, A., Vortex formation in the wake of an oscillating cylinder, *J. Fluids and Structures*, Vol. 2, pp 355-381, 1988.